Analysis of the mesoscopic high cycle multiaxial fatigue strength of fcc metals with crystal plasticity and generalized extreme values probability

Anis HOR[1*], Nicolas SAINTIER[1], Camille ROBERT[2], Thierry PALIN-LUC[1] and Franck MOREL[2]

[1] Arts et Métiers ParisTech, I2M - CNRS, Esplanade des Arts et Métiers 33405 Talence, France
[*] E-mail: anis.hor@ensam.eu.
[2] Arts et Métiers ParisTech, LAMPA, 2 bd du Ronceray 49035 Angers, France

ABSTRACT. *Multiaxial high cycle fatigue modeling of materials is an issue that concerns many industrial domains (automotive, aerospace, nuclear, etc) and in wich many progress still remains to be achieved. Several approaches exist in the litterature: invariants, energy, integral and critical plane approaches all of there having their advantages and their drawbacks. These different formulations are usually based on mechanical quantities at the micro or meso scales using localization schemes and strong assumptions to propose simple analytical forms. This study aims to revisit these formulations using a numerical approach based on crystal plasticity modelling coupled with explicit description of microstructure (morphology and texture). This work has three steps: First, 2D periodic digital microstructures based on a random grain sizes distribution are generated. Multiaxial cyclic load conditions corresponding to the fatigue strength at 10^7 cycles are applied to these microstructures. Then, the mesoscopic Fatigue Indicator Parameters (FIPs), formulated from the different criteria existing in the literature, are identified using the FE calculations of the mechanical fields. These mesoscopic FIP show the limits of the original criteria when it comes to applying them at the grain scale. Finally, a statistical method based on extreme value probability is used to redefine the parameters of these criteria. These new criteria contain the sensitivity of the microstructure variability.*

ABBREVIATION AND DESIGNATION

HCF:	*High Cycle Fatigue*
FIP:	*Fatigue Indicator Parameter*
RVE:	*Representative Volume Element*
SVE:	*Statistical Volume Element*
GEV:	*Generalized Extreme Value distribution*
Microscopic length scale:	*corresponding to the integration points*
Mesoscopic length scale:	*Corresponding to the average density in a grain*
Macroscopic length scale:	*Corresponding to the elementary volume average*

INTRODUCTION

In literature, methods for determining the fatigue behavior based on multiscale modeling estimate that the fatigue strength depends on the extreme value statistics of a single

microstructure attribute [1] (for example inclusion size). This is only valid when the considered element of microstructure is a representative volume element (RVE). A RVE is the smallest volume element whose averaged mechanical behaviour converges towards the macroscopic behaviour of the material. Although the definition of the RVE is possible for some deterministic behaviour aspects (such as elastoplastic behaviour), it is difficult to evaluate a RVE for the HCF strength which is macroscopically highly dispersed. Therefore the use of a single microstructure (with a smaller volume than the RVE with regards to the fatigue behaviour but equal to the RVE size with regards to the elastoplastic behaviour) does not make it possible to take into account the contribution of the microstructural dispersion in the HCF response. To solve this issue, Liao [2] used the Monte Carlo method to build statistical volume element (SVE) of a microstructure with a random distribution of grain sizes and orientations. Despite considering elastic behaviour of crystal only, Liao showed a good correlation between the results obtained by modeling the extreme value probability with a Fréchet distribution and experimental results. Recently, Przybyla et al. [3, 4] introduced a new framework taking into account the effects of neighborhood through the extreme values of the marked correlation functions to quantify the influence of microstructure on the fatigue limit and the contribution of interactions in the microstructure in the case of uniaxial loading. Przybyla used Gumbel distribution function to describe the extreme value probability of the studied parameters.

The purpose of this work is, first, to analyze the microstructure sensitivity (morphology and orientation) of the FIP corresponding to the adaptation of multiaxial fatigue criteria at the mesoscopic length scale. Then a statistical study will be used to define new mesoscopic thresholds for these FIPs, different from the original thresholds of the macroscopic criteria. Finally, the capability of the macroscopic criteria determination to take into account the microstructure sensitivity will be discussed through a comparison between the thresholds determined by the statistical study of the microstructure modeling (called mesoscopic) and the original macroscopic thresholds.

NUMERICAL MODEL

Constitutive relations

The material parameters considered in this work are those of pure copper. This material has a face-centered cubic crystal structure with the reduced number of slip systems (12 <111> {110} slip systems). The behaviour is modeled by cubic elasticity and crystal plasticity constitutive law. The crystal plasticity model used in this work is the one introduced by Meric and Cailletaud [5]. The cubic elasticity constants, the material parameters and the interaction matrix components have been identified on a high purity copper by Gérard et al. [6].

Grain morphology and crystallographic texture

The simulations performed in this work were done using 2D periodic microstructures [7, 8]. The method used to create the topology of the aggregates was based on random distributions in size and shape of ellipses. The CAD model was discretized by 32000 linear triangular finite elements (figure 1-(b)) with the generalized plane strain assumption. Computed microstructure contains 200 equiaxed grains (figure 1-(a)), with an average of 160 finite elements per grain to ensure reasonable computation time. Finally, the random selection of 200 crystal orientations was carried out in the Euler space defined by the three angles ($\varphi_1, \phi, \varphi_2$) assuming cubic crystal symmetry and triclinic sample symmetry. Figure 1-(c) shows the {100} and {110} pole figures of these 200 orientations. Given the low number of orientations, this crystallographic aggregate can be considered as having no preferential orientations.
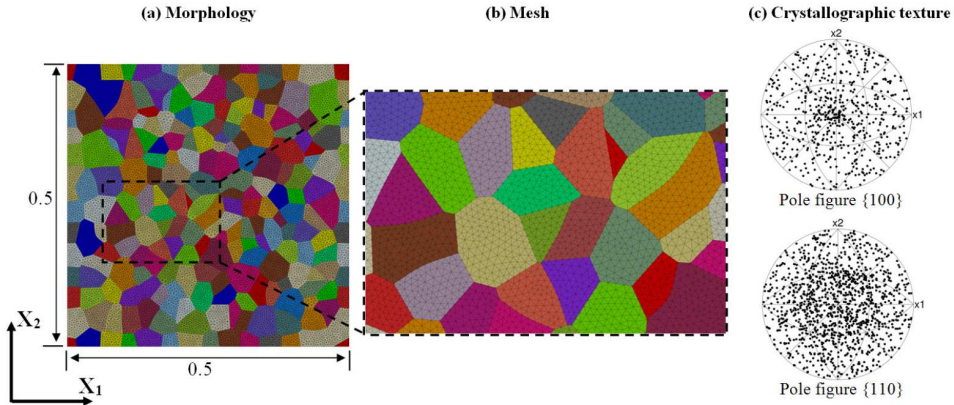
Figure 1. (a) Grain morphology, (b) Mesh and (c) {100} and {110} pole figures showing the selected crystallographic orientations.

Fatigue loading conditions

Different loading conditions are investigated in this section: uniaxial loadings, and tension /torsion loadings with different biaxiality ratios $k = \sigma_a / \tau_a$ and different phase shifts. The selected loading ratio is $R_\Sigma = \sigma_{a,\min} / \sigma_{a,\max} = -1$. The combined loading levels equivalent to the fatigue limit at 10^7 cycles are determined using Crossland criterion [9]. These load levels are given in Table 3.

Table 3. Tension and torsion stress amplitude σ_a / τ_a (MPa) used for different load conditions.

	loading	**Tension**	**Torsion**	**Combined loading tension/torsion**				
	biaxiality	$k = 0$	$k = \infty$	$k = 0.25$	$k = 0.5$	$k = 0.75$	$k = 1$	$k = 2$
Phase shift	$\varphi = 0°$	56/0	0/36	52/13	43.5/22	36/27	30/30	17/34
	$\varphi = 45°$			54/13.5	47/23	38/29	31/31	17/34.5
	$\varphi = 90°$			56/14	56/28	44/33	34/34	17.5/35

MESOSCOPIC FATIGUE INDICATOR PARAMETERS

The studied fatigue indicator parameters (FIPs) were selected from stress criteria widely used in the literature. The multiaxial HCF criteria considered here are Crossland [9], Matake [10] and Dang Van [11]. These fatigue criteria are generally defined in the context of continuum mechanics. In order to evaluate the fatigue criterion on each computed microstructures, the usual HCF criterion are projected on the slip systems of the crystals. This procedure is repeated for each crystal considering its local orientation ($\varphi_1, \phi, \varphi_2$) and stress state computed by FE for each loading case. For instance, the shear stress vector in a given plane is transformed into a resolved shear stress vector over a slip system. The rotation of the crystal in space (defined by the Euler angles ($\varphi_1, \phi, \varphi_2$)) covers all the planes and directions of space, which enables to find the same critical planes and directions (planes and directions maximizing criterion) than those

obtained by the original criterion (with continuous formulation). Table 4 displays the expressions of FIPs adapted to the crystal scale.

Finally, the parameters α_i and β_i describing the median macroscopic threshold of the considered criteria are identified from two median fatigue limits for 10^7 cycles of the considered material smooth specimens under fully reversed loadings: tension ($s_{-1} = 56\ MPa$) and torsion ($t_{-1} = 36\ MPa$) taken from the work of Lukas and Kunz [12]. The parameter β_i is identical for the three criteria ($\beta_c = \beta_m = \beta_{dv} = t_{-1}$). The expression of α_i are also given in Table 4.

Table 4. Expression of Fatigue Indicator Parameters (FIPs) of the studied criteria.

Criterion	I_i	α_i
Crossland	$I_c = \tau^s_{oct,a} + \alpha_c \sigma_{hyd,max} \leq \beta_c$	$\alpha_c = \dfrac{t_{-1} - \left(s_{-1}/\sqrt{3}\right)}{\left(s_{-1}/3\right)}$
Matake	$I_m = \max\limits_{s=1,12}(\tau^s_a) + \alpha_m \sigma_{s,max} \leq \beta_m$	$\alpha_c = 2\dfrac{t_{-1}}{s_{-1}} - 1$
Dang Van	$I_{dv} = \max\limits_{s=1,12}(\max\limits_{t}[\|\hat{\underline{\tau}}^s(s,t)\| + \alpha_{dv}\sigma_{hyd}(t)]) \leq \beta_{dv}$	$\alpha_{dv} = \dfrac{t_{-1} - \left(s_{-1}/2\right)}{\left(s_{-1}/3\right)}$

A comparison between the mesoscopic FIPs predictions and the macroscopic (original) criteria is shown in Figure 2. This comparison shows the existence of grains from which the FIP exceeded the macroscopic threshold. The macroscopic threshold is not applicable at the grain scale. This is especially true for Crossland criterion where most grains are above the threshold. For other criteria, only a small number of grains exceeded the macroscopic threshold. A new mesoscopic threshold can be defined, which corresponds to the line linking the most critical grains (ploted in red in the graphs of figure 2). However, this determination method of the new mesoscopic threshold means that the unique studied elementary volume is representative with regards to fatigue. This hypothesis is not acceptable in the case of a non-deterministic behaviour such as HCF strength. The RVE hypothesis can be replaced by a statistical analysis of the microstructure-sensitivity of the different FIPs. This will be discussed in the next section.
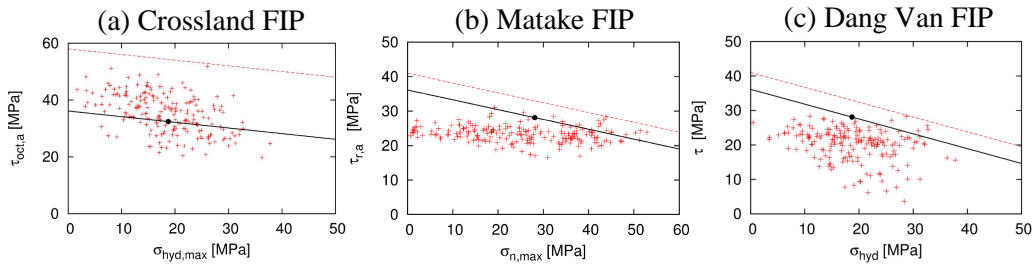

Figure 2. Locus of the 200 FIPs at the grain length scale (red dots), and comparison with the each macroscopic criterion (black dot) in the case of tension loading. The black straight line is the experimental macroscopic threshold and the red straight line corresponds to an effective threshold upper bound for all mesoscopic FIPs determined from a single microstructure.

MICROSTRUCTURE SENSITIVITY

The HCF strength is related to the critical grain whose response leads to the maximum value of the FIP. These extreme values are located at the tails of the density functions of mesoscopic responses and are highly sensitive to the microstructure attributes. To study these critical grains, several statistical approaches are possible. The method selected for this work was based on the extreme value probability.

The extreme value database was constructed by identifying the maximum value of FIP for each statistical colume element (SVE). The number of SVEs was 64: they were obtained by the combination of 8 random morphologies (equiaxed grains) and 8 isotropic textures.

In order to highlight the microstructure sensitivity to the FIPs, a comparison between the mesoscopic predictions corresponding to 64 SVEs and the two thresholds defined above (black and red lines in Figure 3) was performed for tension loading. The black line corresponds to the macroscopic threshold while the red line passing through the critical grain (with the maximum FIP) in the volume element studied previously corresponds to the effective threshold (Figure 2). Figure 3 illustrates this comparison in the case of Crossland FIP. For this criterion the scatterplot (gray dots) exceeded the two thresholds. This observation has motivated the statistical analysis adopted in this work.
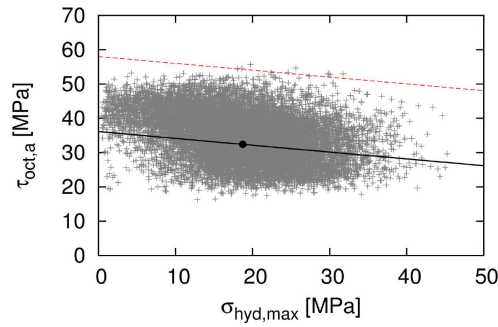

Figure 3. Crossland criterion predictions at the macroscopic length scale (black line) and the mesoscopic length scale (gray dots) for the 64 SVEs and for symmetrical alternated tension loading. The black line is an experimental macroscopic threshold and the red line corresponds to an upper bound effective threshold for all mesoscopic FIPs. This effective threshold correspond to a single VE studied previously (Figure 3).

GENERALIZED EXTREME VALUES PROBABILITY

Let us consider a random variable x with the distribution function $F_X(x)$. The n extreme realizations in n samples of the random variable can be defined as:

$$Y_n = \max(X_1, X_2, ..., X_n) \tag{1}$$

The distribution function of Y_n is defined as:

$$F_{Y_n}(y) \equiv P(Y_n \leq y) = P(X_1 \leq y, X_2 \leq y, ..., X_n \leq y) \tag{2}$$

According to the *Fisher-Tippet theorem*, if there exist two real normalizing sequences $(a_n)_{n \geq 1}$, $(b_n)_{n \geq 1}$ and a non-degenerated distribution (not reduced to a point) G so that:

$$P\left(\frac{Y_n - b_n}{a_n} \leq x\right) = F^n(a_n x + b_n) \xrightarrow[n \to +\infty]{} G(x) \tag{3}$$

G is necessarily one of the three types of distributions: Fréchet, Weibull or Gumbel. Jenkinson [13] combined the three limit distributions in a single parametric form called Generalized Extreme Value (GEV) distribution depending on a single parameter ξ:

$$G_\xi(x) = \begin{cases} \exp\left(-\left(1 + \xi x\right)^{-\frac{1}{\xi}}\right) & si \ \xi \neq 0, \forall x / 1 + \xi x > 0 \\ \exp\left(-\exp(-x)\right) & si \ \xi = 0 \end{cases} \tag{4}$$

The ξ parameter is called extreme index. Its sign indicates the type of asymptotic distribution: Weibull ($\xi < 0$), Gumbel ($\xi = 0$) or Fréchet ($\xi > 0$). The variable $(Y_n - b_n)/a_n$ is called normalized maximum of the random variable x. The parameters a_n and b_n are also called shape factors of the distribution.

We are interested in the maximum values of different FIPs listed in Table 4. Scale factors (a_n and b_n) and extreme index ξ are determined using the maximum likelihood method with a confidence interval of 99%. Figure 4 shows a comparison between the determined distributions and the samples for the Crossland FIP. The identified GEV density function and distribution function showed a good correlation with the probability density and the cumulative probability determined from the extreme values of FIPs database.
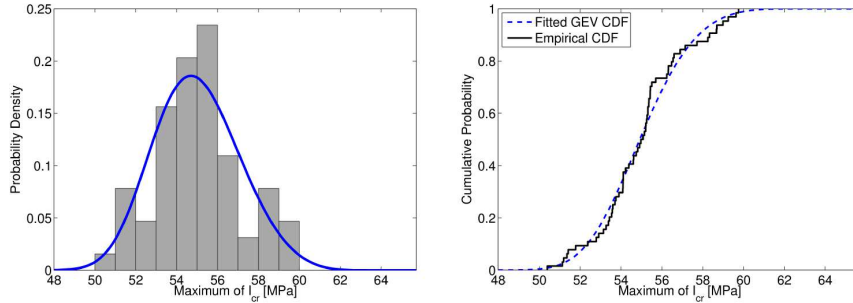

Figure 4. Probability density and cumulative probability determined using the maximum likelihood method from the extreme values of Crossland FIP for tensile loading.

RESULTS AND DISCUSSIONS

Figure 5 represents the mesoscopic thresholds (medians and also the probabilities of 0.1 and 0.9 quantiles) for each loading condition. These factors are normalized by the macroscopic threshold to analyze the effect of microstructure variability. Referring to figure 5, for all studied loading conditions and studied FIPs, the normalized mesoscopic thresholds were always larger

than 1. The adaptation of different studied criteria at the mesoscopic length scale requires increasing this threshold to account for the microstructure variability at this length scale.

On the other hand, the mesoscopic thresholds, defined as the medians of the extreme value distribution of the studied FIPs depend on the loading case. This gap depends on the studied FIP: it is low in the case of the Crossland and Dang Van FIPs (Figure 5-(a) and (c)) and important in the case of the Matake FIP (Figure 5-(b)). For this last FIP, the change in mesoscopic thresholds was observed especially for the biaxial loading with a phase shift of 90°. This difference can be justified by considering that the macroscopic loading levels applied to the polycrystalline aggregate were determined by reference to the Crossland criterion.
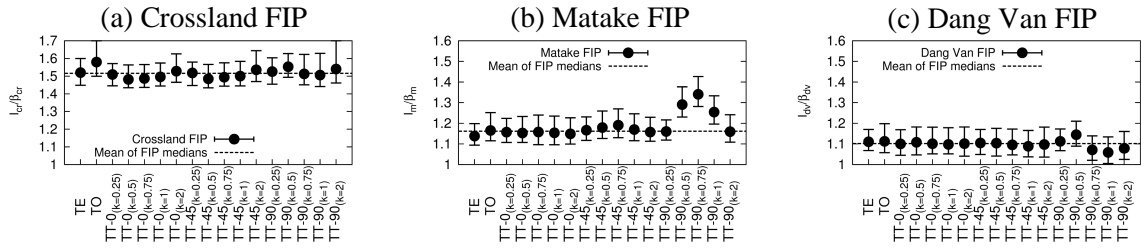

Figure 5. Evolution of the median of the extreme value distributions of (a) Crossland, (b) Matake and (c) Dang Van FIPs, us function of loading conditions. The dots correspond to the median; the two limits of the interval correspond to a probability of 0.10 and 0.90.

Finally, the mesoscopic threshold, common to all loading cases was determined as the average of the thresholds associated to each loading conditions. This mesoscopic average threshold is shown in Figure 5 by the dashed horizontal lines passing through all intervals bounded by the probabilities of 0.1 and 0.9 quantiles in the case of Crossland and Van Dang FIPs. For Matake FIP, this was also true except for the case of biaxial loadings with a phase shift of 90° due to the reasons mentioned above.
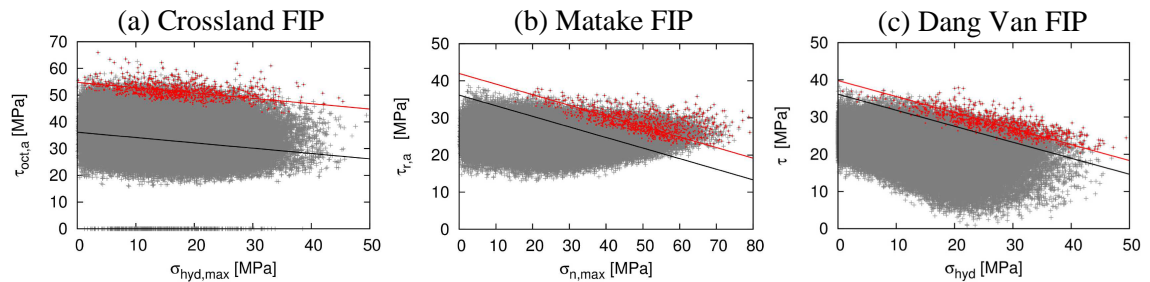

Figure 6. Predictions from (a) Crossland, (b) Matake and (c) Dang Van at the macroscopic length scale (black line) and the mesoscopic length scale (gray dots). The extreme values of these predictions are represented by red dots; the new criteria determined by the average of the medians of the extreme value distributions are represented by the red line.

The mesoscopic threshold of different FIPs is the average (over the different loading conditions) of the medians of the extreme value distributions. Keeping the same value for the α_i parameter, the new criterion containing microstructural heterogeneities contribution at the mesoscopic length scale is plotted in Figure 6. When the mesoscopic threshold (red line) is close to the macroscopic one (black line), the microstructure heterogeneities are taken into account by the

original criterion. This is especially the case of Dang Van criterion and to a lesser extent the case of Matake criterion. For the Crossland criterion, the distance between the two straight lines is important. This comparison proves that critical plane type approaches can capture the microstructure heterogeneity despite simplifying assumptions [11].

CONCLUSIONS

In this work, we analyzed the responses of mesoscopic multiaxial fatigue criteria, widely studied in the literature (Crossland, Matake and Dang Van) from polycrystalline modeling of pure copper coupled with a statistical study of the critical grains. This statistical study allows us to introduce microstructural heterogeneities effect in the variability of the fatigue limits.

The comparison between the mesoscopic predictions of these criteria and the macroscopic (original) criteria shows that they are not conservative at the grain scale. Indeed the identification of macroscopic parameters of these criteria (α_i and β_i) does not take into account the variability due to the microstructure. The solution would be to readjust these parameters on the most critical grain predictions from a calculation. These critical grains are located in the tails of the aggregate response distributions. One of the most used methods to statistically study these critical grains is the extreme value probability. The statistical moment's determination of the different distributions allowed us to define a new mesoscopic threshold for the studied criteria.

These thresholds are the average of the medians of the extreme value distributions related to the different loading conditions. According to the criterion, these thresholds are different or similar to the macroscopic thresholds. For Dang Van, the mesoscopic threshold is close to the macroscopic value of the fatigue indicator parameter (a ratio between the two thresholds is 1.1). At the opposite, for Crossland, the ratio between meso and macro thresholds is greater than 1.5. Matake criterion has a ratio of around 1.2.

Finally, except for the biaxial loading with a phase shift of 90° where FIP median values are very different from one criterion to another, the mesoscopic thresholds is almost the same for all loading conditions. These new mesoscopic thresholds can therefore be determined by applying a single loading case.

REFERENCES

[1]   H.V. Atkinson and G. Shi. Prog. in Mater. Sci., 48: 457-520, 2003.
[2]   M. Liao. Eng. Frac. Mech., 76: 668-680, 2009.
[3]   C. P. Przybyla, R. Prasannavenkatesan, N. Salajegheh, and D. L. Mc-Dowell. Int. J. of Fatigue, 32(3): 512-525, 2010.
[4]   C. P. Przybyla and D. L. McDowell. Int. J. of Plasticity, 26(3): 372-394, 2010.
[5]   L. Meric and G. Cailletaud. J. of Eng. Mater. and Tech., 113(1): 171-182, 1991.
[6]   C. Gérard, F. N'Guyen, N. Osipov, G. Cailletaud, M. Bornert, and D. Caldemaison. Comput. Mater. Sci., 46(3): 755-760, 2009.
[7]   C. Robert, N. Saintier, T. Palin-Luc, and F. Morel. Méca. et Indus., 209-214, 2011.
[8]   C. Robert, N. Saintier, T. Palin-Luc, and F. Morel, Mech. of Mater., 55: 112-129, 2012.
[9]   B. Crossland. Proceedings of the Inter.Conf. on Fatig. of Met., 138-149, London 1956.
[10]   T. Matake. Bulletin of the JSME, 141:257–263, 1977.
[11]   K. Dang Van, B. Griveau, and O. Message. Mech. Eng. Publi. London, 479-496, 1989.
[12]   P. Lukás and L. Kunz. Int. J. of Fatigue, 11(1): 55-58, 1989.
[13]   A.F. Jenkinson. Quaterly Journal of the Royal Meteorological Society, 81, 1955.